J Glob Optim (2007) 38:297–313
DOI 10.1007/s10898-006-9111-3

ORIGINAL PAPER

Use of an interval global optimization tool for exploring feasibility of batch extractive distillation

Erika R. Frits · Mihály Csaba Markót · Zoltán Lelkes · Zsolt Fonyó · Tibor Csendes · Endre Rév

Received: 19 December 2005 / Accepted: 25 October 2006 / Published online: 10 January 2007

Abstract An interval arithmetic based branch-and-bound optimizer is applied to find the singular points and bifurcations in studying feasibility of batch extractive distillation. This kind of study is an important step in synthesizing economic industrial processes applied to separate liquid mixtures of azeotrope-forming chemical components. The feasibility check methodology includes computation and analysis of phase plots of differential algebraic equation systems (DAEs). Singular points and bifurcations play an essential role in judging feasibility. The feasible domain of parameters can be estimated by tracing the paths of the singular points in the phase plane; bifurcations indicate the border of this domain. Since the algebraic part of the DAE cannot be transformed to an explicit form, implicit function theorem is applied in formulating the criterion of bifurcation points. The singular points of the maps at specified process parameters are found with interval methodology. Limiting values of the parameters are determined by searching for points satisfying bifurcation criteria.

Keywords Interval arithmetic · Extractive distillation · Feasibility · Bifurcation

E. R. Frits · Z. Lelkes · Z. Fonyó · E. Rév (✉)
Dept. Chemical Engineering, Budapest University of Technology and Economics, P. O. Box 91, 1521, Budapest, Hungary
e-mail: ufo@mail.bme.hu

E. R. Frits (✉) · Z. Fonyó · E. Rév
HAS–BUTE Research Group of Technical Chemistry, P. O. Box 91, 1521, Budapest, Hungary
e-mail: efrits@mail.bm.hu

M. C. Markót
Computer and Automation Research Institute, Hungarian Academy of Sciences, P. O. Box 63, 1518, Budapest, Hungary
e-mail: markot@sztaki.hu

T. Csendes
University of Szeged, Institute of Informatics, P. O. Box 652, 6701, Szeged, Hungary,
e-mail: csendes@inf.u-szeged.hu

1 Batch extractive distillation and elements of the feasibility study

Distillation as a process used for separating liquid components is based on volatility difference between the components to be separated. Volatility depends on temperature, pressure, and the composition of the mixture. The liquid mixture is boiled; the more volatile component has a greater fraction in the emerging vapor than in the liquid. Repeated boiling and condensation produces a set of liquid and vapor streams flowing counter-current way in a distillation column. The components are enriched at the two ends of the column.

At given pressure the boiling temperature depends on the liquid composition. Volatility depends heavily on composition in case of mixtures that behave in a strongly non-ideal way. Some component pairs exhibit identical volatility at a certain composition, called **azeotrope**. Since boiling such a mixture produces vapor of identical composition, the components cannot be separated in this way. Well known examples are: ethanol and water, acetone and methanol, chloroform and ethyl acetate, toluene and methanol, etc.

Extractive distillation processes apply a third component, the so-called entrainer, to make the separation feasible. There are several variants of these processes according to the volatility relations between the components, and according to the several technical opportunities to be chosen. A usual configuration is shown in Fig. 1. This is a batch process, i.e., this process works up a given finite charge of mixture of components A and B to be separated. The process itself is a semi-batch or fed-batch nature in the sense that entrainer E is pumped to the system continuously during the separation step of the process.

The charge is loaded to the boiler (vessel) situated at the bottom of the column. This vessel is also called "*the still*." The composition in the still will be denoted by $\mathbf{x}_S$ ($\mathbf{x}$ is an array of mole fractions, and $\mathbf{x}_S$ is the array of mole fractions in the still).

The still is boiled, and vapor stream of flow rate V is driven through the column. The vapor emerging from the top of the column is condensed. A part of the condensate, with flow rate L, is led back to the top of the column. The other part of the condensate is removed as **distillate**, with flow rate D. Its composition is denoted by $\mathbf{x}_D$. An important parameter of the process is the **reflux ratio** $R = L/D$. When no

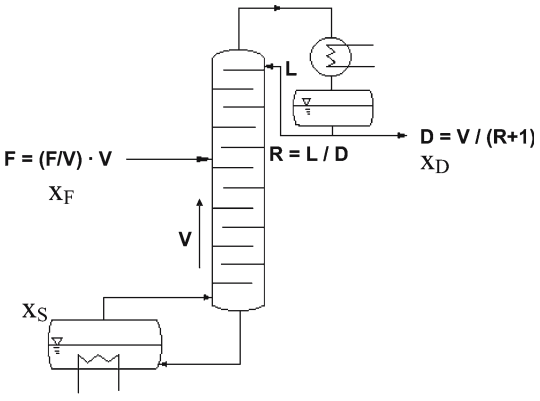

Fig. 1 BED in a rectifier

distillate is removed but all the condensate is led back as reflux (i.e., when $D = 0$ and $L = V$), we speak about **total reflux**.

The entrainer stream is pumped to the column with flow rate F; its composition is denoted by $\mathbf{x}_F$. The entrainer stream usually consists of pure component E; its composition is $\mathbf{x}_F = [0, 0, 1]$. (Composition anywhere in the system is denoted by an array of the mole fractions x_A, x_B, and x_E. Thus, the above value of composition $\mathbf{x}_F$ should be read as $x_{AF} = 0$, $x_{BF} = 0$, and $x_{EF} = 1$. These letters represent mole fraction of component A in stream F, mole fraction of component B in stream F, and mole fraction of component E in stream F, respectively. Since the sum of mole fractions should give unity, two of them are sufficient to determine the composition.) **Feed ratio** F/V is another important parameter of the process. The feed is related to the vapor stream because the boiling power is usually constant for technical reasons, and this gives rise to approximately constant vapor flow rate in time.

Production of components in specified purity and acceptable recovery is possible if the process parameters are kept in a so-called **feasible domain**. This domain is not known in advance. Random trials usually result in finding the process infeasible, even if it is feasible with appropriate parameters. The feasibility methodology suggested by Lelkes et al. [1], and successfully applied, e.g., by Lelkes et al. [2] and Rév et al. [3], is a procedure used for determining the feasible domain by systematic analysis of the phase maps of DAEs that are set up as an approximate model of the process.

2 Model equations and phase map analysis

The differential equation describing the change of mole fractions $\mathbf{x}$ along the column at a given time instant is

$$\frac{\mathrm{d}\mathbf{x}}{\mathrm{d}h} = \frac{V}{L}\left(\mathbf{y}(\mathbf{x}) - \mathbf{y}^*(\mathbf{x})\right), \tag{1}$$

where h is an internal running variable, $\mathbf{y}^*(\mathbf{x})$ and $\mathbf{y}(\mathbf{x})$ are multivariate functions. The latter has two forms depending on which section of the column is modeled. Its form in the upper section is

$$\mathrm{y} = \frac{R}{R+1}\mathbf{x} + \frac{1}{R+1}\mathbf{x}_D, \tag{2}$$

whereas its form in the lower section is

$$\mathbf{y} = \left(\frac{R}{R+1} + \frac{F}{V}\right)\mathbf{x} + \frac{1}{R+1}\mathbf{x}_D - \frac{F}{V}\mathbf{x}_F. \tag{3}$$

$\mathbf{y}^*(\mathbf{x})$ is determined by the following system of Eq. 4—10:

$$y_i^* P = \gamma_i x_i p_i^\circ \quad (i \in \{A, B, E\}), \tag{4}$$

$$\log_{10} p_i^\circ = A_i - \frac{B_i}{T - 273.14 + C_i} \quad (i \in \{A, B, E\}), \tag{5}$$

$$\ln \gamma_i = \frac{\sum\limits_{j\in\{A,B,E\}} \tau_{ji} G_{ji} x_j}{\sum\limits_{l\in\{A,B,E\}} G_{li} x_l} + \sum_{j\in\{A,B,E\}} \frac{x_j G_{ij}}{\sum\limits_{l\in\{A,B,E\}} G_{lj} x_j} \left(\tau_{ij} - \frac{\sum\limits_{n\in\{A,B,E\}} x_n \tau_{nj} G_{nj}}{\sum\limits_{l\in\{A,B,E\}} G_{lj} x_j} \right) \quad (i \in \{A,B,E\}) \tag{6}$$

$$\tau_{ij} = \frac{U_{ij}}{R_G T} \quad (i,j \in \{A,B,E\}), \tag{7}$$

$$G_{ij} = \exp\left(-\alpha_{ij}\tau_{ij}\right) \quad (i,j \in \{A,B,E\}). \tag{8}$$

$$\sum_{i\in\{A,B,E\}} y_i^* = 1. \tag{9}$$

Here R_G=1.98721 is a universal constant; $U_{ij}, \alpha_{ij} = \alpha_{ji}, A_i, B_i, C_i (i,j \in \{A,B,E\})$, and P are model parameters amongst which P is the system's pressure (measured in Hg mm), the others are parameters of the thermodynamic model. The mole fractions x_A and x_B are independent variables; T(boiling temperature), γ_i (activity coefficient), p_i^0 (pure component's vapor pressure), and the auxiliary variables τ_i, and G_{ij} $(i,j \in \{\mathrm{A, B, E}\})$ are dependent variables. Mole fraction of the entrainer component x_E depends on x_A and x_B at any composition via normalization:

$$\sum_{i\in\{A,B,E\}} x_i = 1. \tag{10}$$

The methodology is demonstrated using the above system of equations, and a particular set of parameter values given in Tables 1 and 2. These parameters describe the material system of acetone (component A), methanol (component B), and water (component E) at atmospheric pressure ($P = 760\,\mathrm{Hg\,mm}$). Methanol and acetone form an azeotropic mixture (called an 'azeotrope') at $x_{\mathrm{acetone}} \approx 0.821$, at this pressure. All over our study, the specified distillate composition is $\mathbf{x}_D = [0.94, 0.025, 0.035]$ (acetone, methanol, water). Pure water is applied in the entrainer feed, i.e., $\mathbf{x}_\mathrm{F} = [0.0, 0.0, 1.0]$. Two sub-problems are considered. One is the properties of the phase curve of the solution of the DAE

$$(1),\ (2),\ \text{and}\ (4)\text{–}(10) \tag{RP}$$

and the other one is the phase map properties of the DAE

$$(1), (3),\ \text{and}\ (4)\text{–}(10). \tag{EP}$$

Solution of RP with $\mathbf{x}_D$ as initial value has a single projection to the phase space $[x_\mathrm{A}, x_\mathrm{B}]$. This projection is called *the rectifying profile*.

The still composition $\mathbf{x}_S$ (see also Fig. 1) is not known; moreover, it changes with time. Thus, a solution is computed to each supposed $\mathbf{x}_S$ by solving EP with $\mathbf{x}_{\mathrm{initial}} = \mathbf{x}_S$ as initial value, and they are also projected to the phase space $[x_\mathrm{A}, x_\mathrm{B}]$. These projections are called *extractive profiles*. Thus, a phase map consisting of the single rectifying profile and a set of extractive profiles is formed. The map of the extractive profiles, without considering the rectifying profile, is called *the extractive profiles' map*.

Table 1 Parameters A_i, B_i, and C_i

i	A_i	B_i	C_i
A	7.11714	1210.595	229.664
B	8.08097	1582.271	239.726
E	8.07131	1730.63	233.426

Table 2 Parameters U_{ij}, and α_{ij}

i	j	U_{ij}	U_{ji}	$\alpha_{ij} = \alpha_{ji}$
A	B	399.395	−16.784	0.292
A	E	−47.613	1919.523	0.291
B	E	−347.817	−347.817	0.302

The physically interpretable phase domain is a triangle in the plane of x_A and x_B. (The vertices are [0,0], [1,0], and [0,1] in the plane; these correspond to the composition arrays [0,0,1], [1,0,0], and [0,1,0], respectively.)

A necessary condition of process feasibility is that the extractive profiles connect all the still compositions $\mathbf{x}_S$ to the rectifying profile as $\mathbf{x}_S$ moves in the triangle during the process.

The still vessel contains the residue after distillation. The farther $\mathbf{x}_S$ moves from vertex A, the less amount of component A remains in the residue, and the greater recovery of component A is reached. The process is feasible even if a small recovery can be reached, but great recovery is targeted. Thus, how far $\mathbf{x}_S$ can be moved is also an important aspect.

Singular points of the extractive profiles' map play a key role in assessing feasibility and estimating maximum recovery.

Singular points of the DAE are classified in this article according to the usual convention in the literature. Our equations are autonomous, and do not have periodic solution. (Non-existence of any periodic solution follows from thermodynamics.) A singular point is called stable if all the phase curves approach it from its neighborhood, and called unstable if they approach it from the neighborhood when computed in opposite direction, which can be accomplished by changing the sign of the right-hand side of the differential equations. Saddles have two approaching solutions and two solutions going away in their neighborhood, together with four separated phase curve bundles of hyperbolic nature. Other (degenerate) solutions do not occur, unless in bifurcation points. We speak about bifurcation when the map topology suddenly changes in function of the parameters [4, 5]. Points where singular points appear, disappear, or change type are called bifurcation points.

An example phase map is shown in Fig. 2. The task is separating acetone (A) from methanol (B), with water as entrainer (E). The applied parameters are $R = 4$, and $F/V = 0.58$.

Here an unstable node UN of the extractive profiles' map is situated near vertex E, and a saddle point S_2 is found well inside the triangle. (Our notation originates from the relevant literature of these chemical systems [1].) Two bundles of extractive profiles come from UN along the separatrix from UN toward S_2. One of them turns toward the BE edge, the other one turns toward stable node SN. This SN must exist somewhere outside the triangle; but the bundle of extractive profiles is dense enough

near the base to illuminate a node on the edge. The other two bundles around S_2 come from the direction of the AB edge, and their destination is the same as those coming from UN. Another unstable node must also exist somewhere outside the triangle, over its AB edge.

This is a map of a feasible process because the $\mathbf{x}_S$ composition can move from the AB edge near vertex A up to the two stable separatrices of S_2, and all the extractive profiles along its path cross the rectifying profile. In other words, all the points of the triangle to the right from those two separatrices are feasible still compositions. The points on, and to the left of, the stable separatrices of S_2 cannot serve as feasible still compositions because the extractive profiles computed from them do not reach the rectifying profile.

Thus, these two separatrices form a boundary to the feasible still composition. The distillate composition $\mathbf{x}_D$ cannot be kept at its specified value when $\mathbf{x}_S$ reaches and crosses this boundary, but it also moves farther from vertex A. Production of distillate is stopped at this moment, and some amount of component A remains in the still. Thus, perfect recovery of A cannot be achieved with this process.

The appropriate process parameters can be estimated by computing and analyzing the phase maps with systematically changed parameter values. Location of the singular points, and the parameter values at which some singular points appear or disappear, play a key role in assessing feasibility. For example, the process with the given parameters is qualified feasible according to the phase map in Fig. 2 because the stable node SN is situated below the AE edge. SN is situated inside the triangle at small *F/V* value, and the extractive profiles do not cross the rectifying profile in that case. The map changes with R, as well. Location of S_2 is also influenced by R and F/V.

The singular points, especially the saddle points, cannot always be determined with satisfactory precision; moreover, some details of the map are missed because unstable nodes are not determined, and singular points out of a physically interpretable region are not studied. Bifurcation cannot always be recognized because the computed maps are not detailed enough. Existence of a singular point cannot be excluded merely on the basis of not finding it with a given mesh over the studied domain. In contrast to this lack of information, interval arithmetic has the potential of excluding the existence of some solutions, and finding the bifurcation points according to their mathematical criteria.

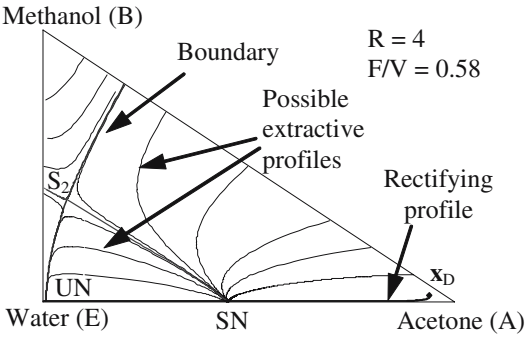

Fig. 2 Phase map at $R = 4$ and $F/V = 0.58$

3 Interval methodology

For our engineering problems we decided to use an available interval optimization tool, the one recently developed at the University of Szeged. The algorithm itself is an improved version of the branch-and-bound global optimization procedure of the C-XSC Toolbox [6], and it is implemented using the Profil/BIAS interval arithmetic library of Knüppel [7]. The interval inclusion functions are evaluated with a combination of the natural interval extension and a first-order centered (mean-value) form [8]. The accelerating tools are the monotonicity, mid-point, cut-off, and concavity tests, and a step of the interval Newton–Gauss–Seidel iteration, all discussed in [6]. The interval subdivision rule is the one named as 'C/3' in [9]. This rule means that each actual interval is subdivided to have three subintervals in the direction for which the range of the objective value changes the most within the respective interval. The stopping criterion of the algorithm is based on the width of the actual box: if each component's width is smaller than a prescribed value (10^{-2}–10^{-12}, depending on the particular application) then the box is inserted to the list of candidate enclosures for the global minimizers.

Beside the basic branch-and-bound procedure, the algorithm contains a verification procedure [10] based on the interval Newton-step in order to check the existence and local uniqueness of the candidate optimizers. Further details of the algorithm can be found in [9,11]. Global optimization algorithms can be applied to solve both minimization problems and root finding problems, because any root-finding problem

$$f_i(x_1, x_2, \ldots, x_N) = 0 \quad (i = 1, 2, \ldots, N) \tag{11}$$

can be re-formulated as an optimization problem

$$\min_{\mathbf{x}} \sum_{i=1}^{N} f_i^2(\mathbf{x}). \tag{12}$$

If (11) has a solution then it is a (global) minimizer of (12) because the sum of squares cannot be negative. That is, if the global minimum of (12) is guaranteed to be positive over a given search domain then (11) has no solution over the same domain. All over our study we apply this re-formulation for determining zeroes of equations.

Singular points can be computed even outside the composition triangle; this opportunity is constrained to a small neighborhood around the triangle because of the mathematical form of the model. Thus, we searched for singular points till $x_{\text{Methanol}} = -0.1$; but no farther.

The numerical computations were run on a Pentium IV PC (with 1 Gbyte of RAM and a 1.4 GHz CPU) under Linux operating system.

4 Singular points

Singular points of (RP) and (EP) are characterized by a zero value of the differentials in Eq. 1. This is fulfilled when the right-hand side equals zero, i.e., when

$$\frac{V}{L}\left(\mathbf{y}(\mathbf{x}) - \mathbf{y}^*(\mathbf{x})\right) = \mathbf{0}. \tag{13}$$

Thus, singular points of (RP) satisfy the following algebraic equation system:

$$(2), (4)\text{–}(10) \text{ and } (13). \tag{SRP}$$

Singular points of (EP) satisfy the following algebraic equation system:

$$(3)\text{–}(10) \text{ and } (13). \tag{SEP}$$

4.1 Singular points of (RP)

Singular points of RP are searched in order to determine the minimum value of R above which the phase curve of RP, i.e., the rectifying profile, is long enough to cross the extractive profiles arriving to the stable node. The length of the profile has a sudden jump at this value.

Values of $U_{ij}, \alpha_{ij} = \alpha_{ji}, A_i, B_i, C_i (i,j \in \{A,B,E\}), R_G, P$, and R are given; values of $\gamma_I, p_i^0 \tau_i, G_{ij}, x_i, y_i, y_i^*, (i,j \in \{A,B,E\}), x_E$ and T are unknown. Equation system SRP is transformed to a global minimization problem. The independent variables are $x_\mathrm{A}, x_\mathrm{B}$, and T. The searched box is {[0,1], [0,1], [200, 500]}. (Temperature is measured in Kelvin.) The depending variables are expressed and substituted. The objective function is

$$\sum_{i \in \{A,B,E\}} \left(y_i(\mathbf{x}) - y_i^*(\mathbf{x})\right)^2 + (x_A + x_B + x_E - 1)^2, \tag{14}$$

where x_E could be expressed as $x_\mathrm{E} = 1 - x_\mathrm{A} - x_\mathrm{B}$ and substituted to the constraint system, but the argument of the logarithms in Eq. 5 and 6 could easily become negative during the search in that case because interval arithmetic is used. That is why the second member appears in the objective function.

Several solution problems are formed by varying R.

Solutions of (SRP) are found relative easily by the solver. The present interval tool is able to find all the singular points at any specified R, except very near the bifurcation points. As a result, a bifurcation diagram is plotted and shown in Fig. 3. The squares, lined up along imagined curves of negative slope, represent stable points; the same is true for points denoted with diamonds. The triangles, lined up along an imagined curve of positive slope, represent unstable points. Since the phase curve of RP is started from $\mathbf{x}_\mathrm{D}$, it does not run below $x_\mathrm{A} = 0.7$ if R is smaller than 0.629, but stops at the upper stable point. At $R > 0.63$, however, the phase curve reaches below $x_\mathrm{A} = 0.1$, a stable point in the lower curve.

Earlier we tried to explore the situation via subsequently solving SRP using GAMS/CONOPT [12,13] with varying R. We could not find the instable nodes in that way. Instead, we found the solutions represented by diamonds, at $R < 0.6$.

All the points shown in Fig. 3 are found with this interval method **except** the rightmost square at about $R \approx 0.63$ and $x_\mathrm{Acetone} \approx 0.7$. The nearer R is specified to this value, the longer time is consumed by the solver. The reason of this phenomenon must be that we encounter a bifurcation here.

4.2 Singular points of (EP)

Values of $U_{ij}, \alpha_{ij} = \alpha_{ji}, A_i, B_i, C_i (i,j \in \{\mathrm{A, B, E}\}), R_G, P, R$, and F/V are given; values of $\gamma_i, p_i^0, \tau_i, G_{ij}, x_i, y_i, y_i^*, (i,j \in \{\mathrm{A, B, E}\}), x_E$, and T are unknown. Equation system SEP is transformed to a global minimization problem. The independent variables,

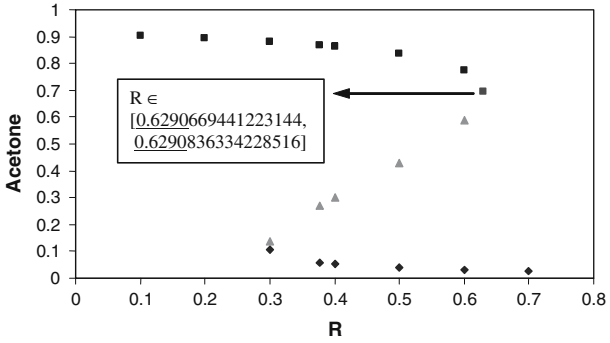

Fig. 3 Plot of x_{Acetone} component of the found singular points in function of R

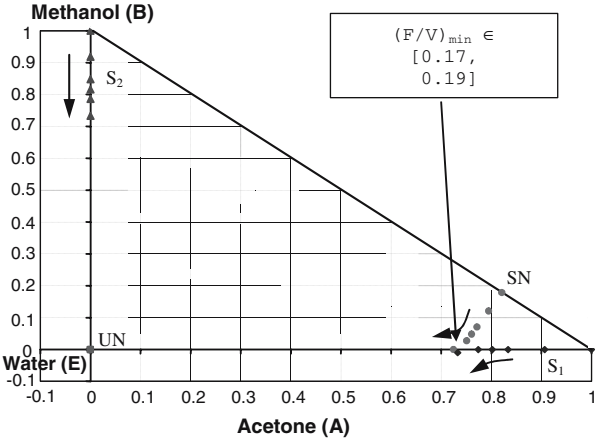

Fig. 4 Singular point paths with evolving F/V at total reflux

the searched box, and the objective function are the same as in the case of SRP. The depending variables are expressed and substituted. Several solution problems are formed by varying R (between 0.1 and 10.0) and F/V (between 0 and 1.0).

Solutions of (SEP) are also found relative easily by the solver. Series of solutions with changing F/V at fixed R are shown in the subsequent figures. These results are interesting in the sense they reveal how the location of bifurcation changes with R. Earlier we thought that the critical value of F/V can be determined by computing when the stable node SN reaches the base line (the AE edge). This is, however, valid at total reflux only. This total reflux case is shown in Fig. 4. Four singular points of the map are located in the arbitrary small neighborhoods of the three vertices, and the arbitrary small neighborhood of the azeotrope, if F/V approaches zero. These points are shifted with increasing F/V as it is shown in Fig. 4. The singular points are determined by stepwise incrementing F/V. The stable node originated from the azeotrope moves toward the AE edge and meets just at the edge another point (S_1) originated from the acetone vertex. At higher values the stable point moves on the same edge toward the water vertex. Thus, the minimum feed ratio is approximately 0.19 if total reflux is applied.

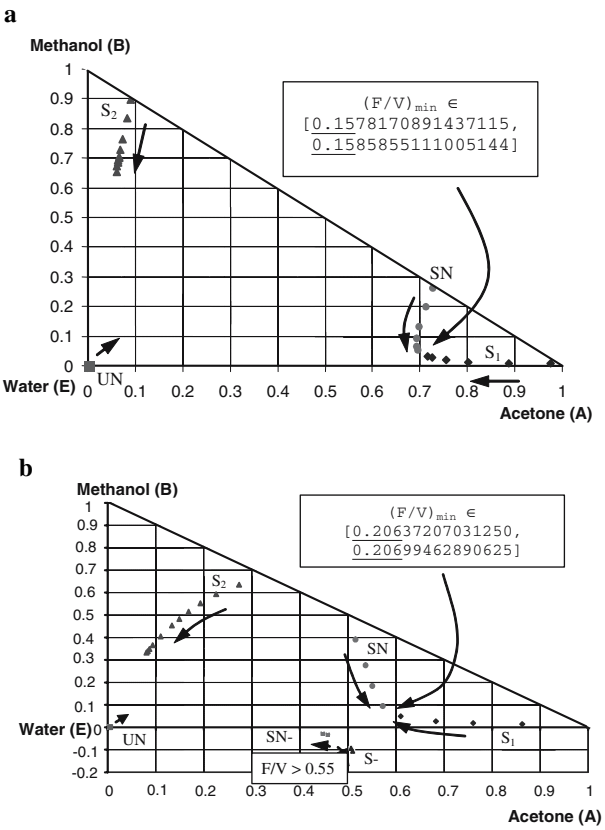

Fig. 5 **(a)** Singular point paths with evolving F/V at $R = 10$ **(b)** Singular point paths with evolving F/V at $R = 4$

All the singular points move in the interior of the triangle at decreasing R. How the singular points move in the triangle is shown in Fig. 5 with $R = 10$, $R = 4$. Unstable node UN originated from the water vertex is shifted so little that it practically remains located there. Stable node SN does not start from the azeotrope, but seems coming from a point on the acetone/methanol edge, between the azeotrope and the methanol vertex. Saddle S_1, originated from the acetone vertex, does not move on the base line. SN and S_1 meet at an F/V depending on R.

There is a bifurcation at $F/V \approx 0.207$ if $R = 4$ is specified (Fig. 5b). Above this value a wide bundle of curves are directed toward a point somewhere outside the triangle. Thus, the minimum feed ratio is $F/V \approx 0.207$ if $R = 4$ is applied. The stable node originated from the azeotrope does not reach the acetone/water edge. A second bifurcation happens at $F/V \approx 0.55$. A new stable point SN− appears outside the composition triangle and moves toward the water vertex. There is also another saddle S−, as its counterpart, but not shown in the figure. This new bifurcation has no effect on the feasibility of the process.

All the mentioned singular points are determined with the present interval tool with stepwise incremented F/V parameters. The bifurcation points cannot be exactly determined in this way. The nearer F/V is specified to this value, the longer time is consumed by the solver. The reason of this phenomenon must be that we encounter a bifurcation here.

5 Bifurcation points

Those parameter values at which the bifurcations occure constitute the border of the feasible domain. However, computation work consumed for finding the singular points increases when the bifurcation points are approached.

Bifurcation points can be approximately determined via computing singular points and plotting bifurcation diagrams. Such diagrams are shown in Fig. 6a–c for our problem. Reliable computation of bifurcations is, however, the target of this section.

Acetone mole fractions of SN and S_2 are plotted against F/V at specified R in Fig. 6a–c. The curves do not meet exactly, but they have to do so at higher F/V. Note also that singular points far outside the triangle are not computed; that is why some sequences are imperfect. A saddle point is missing, for example, in Fig. 6c at high F/V.

The meeting point could not be well approximated by simply determining the singular points with stepwise incremented feed ratio, as mentioned in Sect. 4.2, because the computation time increases to infinity as the bifurcation point is approximated. Instead, the criterion of bifurcation is applied as a new constraint in the model.

The character of a singular point can be analyzed by linearizing the differential equation in its neighborhood [4,5,14,15].

Accordingly, Eq. (1) is approximated by

$$\frac{\mathrm{d}\mathbf{x}}{\mathrm{d}h} = \mathbf{A}\mathbf{x}, \tag{15a}$$

where matrix $\mathbf{A}$ is the *Jacobian* computed at the *singular* point $\mathbf{x}$:

$$a_{ij} = \frac{\partial}{\partial x_j}\left(\frac{V}{L}\left[y_i(\mathbf{x}) - y_i^*(\mathbf{x})\right]\right)\Bigg|_{\mathrm{x}} \quad (i \in \{A,B\},\ j \in \{A,B\}). \tag{15b}$$

Singular points that are not bifurcation points are characterized by non-zero real part in each eigenvalue of the coefficient matrix $\mathbf{A}$. Bifurcation points are characterized by at least one eigenvalue with zero real part [4,5,14,15]. Only simple singular points that are characterized with only real eigenvalues occur in our case and, consequently, irregularity is simply indicated by a zero determinant of $\mathbf{A}$. In this case, the criterion of bifurcation is:

$$\det(\mathbf{A}) = 0. \tag{16}$$

Thus, the equation system to be solved is the following:

$$(3)\text{–}(10), (13), \text{ and } (16) \tag{17}$$

with F/V considered as a variable, while R is fixed.

However, the entries of the *Jacobian* (Eq. 15b) cannot be simply computed, because the function to be differentiated by x_A and x_B cannot be expressed in them. This is because variable T (the boiling temperature) cannot be algebraically discarded. In practice, we have the following relations:

$$\begin{aligned} a_{\mathrm{AA}} &= \tfrac{\partial}{\partial x_\mathrm{A}} f_\mathrm{A}(x_\mathrm{A}, x_\mathrm{B}, T)\Big|_{x_\mathrm{A},x_\mathrm{B}} & a_{\mathrm{AB}} &= \tfrac{\partial}{\partial x_\mathrm{B}} f_\mathrm{A}(x_\mathrm{A}, x_\mathrm{B}, T)\Big|_{x_\mathrm{A},x_\mathrm{B}}, \\ a_{\mathrm{BA}} &= \tfrac{\partial}{\partial x_\mathrm{A}} f_\mathrm{B}(x_\mathrm{A}, x_\mathrm{B}, T)\Big|_{x_\mathrm{A},x_\mathrm{B}} & a_{\mathrm{BB}} &= \tfrac{\partial}{\partial x_\mathrm{B}} f_\mathrm{B}(x_\mathrm{A}, x_\mathrm{B}, T)\Big|_{x_\mathrm{A},x_\mathrm{B}}, \end{aligned} \tag{18}$$

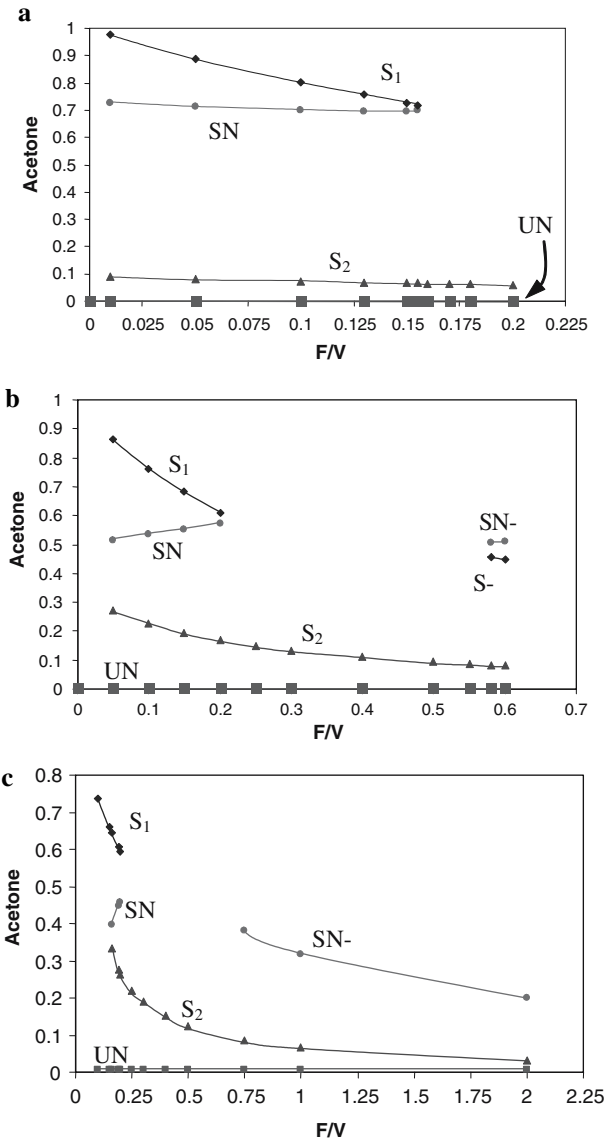

Fig. 6 **(a)** Bifurcation diagram at $R = 10$ **(b)** Bifurcation diagram at $R = 4$ **(c)** Bifurcation diagram at $R = 3$

where T is an implicit function of x_A and x_B. An imagined explicit form is denoted by ϑ:

$$T = \vartheta\,(x_A, x_B)\,. \tag{19}$$

In order to determine the partial derivatives, the chain rule can be applied:

$$a_{ij} = \left.\frac{\partial f_i(\mathrm{x}, T)}{\partial x_j}\right|_{\mathbf{x}, T=\vartheta(\mathbf{x})} + \left.\frac{\partial f_i(\mathbf{x}, T)}{\partial T}\right|_{\mathbf{x}, T=\vartheta(\mathbf{x})} \times \left.\frac{\partial \vartheta(\mathbf{x})}{\partial x_j}\right|_{\mathbf{x}} \quad (i \in \{A, B\},\ j \in \{A, B\}). \tag{20}$$

The above partial derivatives of f_i according to the mole fractions can be expressed analytically, as follows.

$f_i(\mathbf{x}, T)$ is a function of $\mathbf{x}$ and T, but T depends implicitely on $\mathbf{x}$. Thus, $f_i(\mathbf{x}, T)$ is a variant of $\widehat{f}_i(\mathbf{x})$

$$\hat{f}_i(\mathbf{x}) = \frac{V}{L}\left[y_i(\mathbf{x}) - y_i^*(\mathbf{x})\right] \quad (i \in \{A, B\},\ j \in \{A, B\}). \tag{21}$$

where the dependence on T is eliminated.

Thus, elements of the *Jacobian* can be expressed as

$$a_{ij} = \left.\frac{\partial y_i(\mathbf{x})}{\partial x_j}\right|_{\mathbf{x}} - \left(\left.\frac{\partial g_i(x, T)}{\partial x_j}\right|_{\mathbf{x}, T=\vartheta(\mathbf{x})} + \left.\frac{\partial g_i(x, T)}{\partial T}\right|_{\mathbf{x}, T=\vartheta(\mathbf{x})} \times \left.\frac{\partial \vartheta(x)}{\partial x_j}\right|_{\mathbf{x}}\right), \quad i \in \{A, B\},\ j \in \{A, B\}, \tag{22}$$

where y_i^* is expressed as a function $y_i^* = g_i(x_\mathrm{A}, x_\mathrm{B}, T)$:

$$g_i(x_\mathrm{A}, x_\mathrm{B}, T) = \frac{\gamma_i(x_\mathrm{A}, x_\mathrm{B}, T)\, x_i p_i^0(T)}{p} \quad i \in \{A, B\} \tag{23}$$

The actual vapor composition $\mathbf{y}$ expressed in the form of (3) does not depend on temperature. Function $g_i(\mathbf{x}, T)$ is used to express $\mathbf{y}^*$ in function of $\mathbf{x}$ and the explicitly unknown T which in turn depends on $\mathbf{x}$ via ϑ.

The derivatives of $\mathbf{y}$ are given by

$$\frac{\partial y_i}{\partial x_j} = \begin{cases} 0, & i \neq j, \\ \frac{R}{R+1}, & i = j, \end{cases} \quad i \in \{A, B\},\ j \in \{A, B\}. \tag{24}$$

In order to determine the derivatives of $y_i^*(\mathbf{x})$, expressed as in (24), $g_i(x_\mathrm{A}, x_\mathrm{B}, T)$ should be differentiated according to its arguments:

$$\frac{\partial g_i}{\partial x_j} = \frac{p_i^0(T)}{p} \cdot \begin{cases} x_i \frac{\partial \gamma_i(\mathbf{x}, T)}{\partial x_j}, & i \neq j \\ x_i \frac{\partial \gamma_i(\mathbf{x}, T)}{\partial x_j} + \gamma_i(\mathbf{x}, T) & i = j \end{cases} i, j \in \{A, B\} \tag{25}$$

$$\frac{\partial g_i}{\partial T} = \frac{x_i}{p}\left(p_i^0(T)\frac{\partial \gamma_i(\mathbf{x}, T)}{\partial T} + \gamma_i(\mathbf{x}, T)\frac{\partial p_i^0(T)}{\partial T}\right), \quad i \in \{A, B\}. \tag{26}$$

The sum of the mole fractions should equal unity; this condition is applied to eliminate one of the mole fractions:

$$x_E = 1 - \sum x_k \quad k \in \{A, B\}, \tag{27}$$

Equations 25 and 26 contain the partial derivatives of Eq. 5 and 6, respectively:

$$\frac{\partial p_i^0}{dT} = 10^{\left(A_i - \frac{B_i}{T - 273.14 + C_i}\right)} \cdot \frac{B_i \cdot \ln(10)}{(T - 273.14 + C_i)^2} = p_i^0 \frac{B_i \cdot \ln(10)}{(T - 273.14 + C_i)^2}, \tag{28}$$

$$\frac{\partial \gamma_i}{\partial T}=\gamma_i \left(\begin{array}{l} \frac{\sum_j x_j \left(\frac{\partial \tau_{ji}}{\partial T} G_{ji}+\frac{\partial G_{ji}}{\partial T}\tau_{ji}\right)\cdot\sum_k G_{ki}x_k-\sum_j x_j \tau_{ji} G_{ji}\cdot\sum_k x_k \frac{\partial G_{ki}}{\partial T}}{\left(\sum_k G_{ki}x_k\right)^2}+ \\ +\sum_j x_j \frac{\left(\frac{\partial \tau_{ij}}{\partial T} G_{ij}+\frac{\partial G_{ij}}{\partial T}\tau_{ij}\right)\cdot\sum_k G_{kj}x_k-\tau_{ij}G_{ij}\sum_k x_k \frac{\partial G_{kj}}{\partial T}}{\left(\sum_k G_{kj}x_k\right)^2}- \\ -\sum_j x_j \frac{\left(\frac{\partial G_{ij}}{\partial T}\sum_m x_m \tau_{mj}G_{mj}+G_{ij}\sum_m x_m\left(\frac{\partial \tau_{mj}}{\partial T}G_{mj}+\frac{\partial G_{mj}}{\partial T}\tau_{mj}\right)\right)\cdot\left(\sum_k G_{kj}x_k\right)-2G_{ij}\sum_m x_m\tau_{mj}G_{mj}\cdot\sum_k x_k\frac{\partial G_{kj}}{\partial T}}{\left(\sum_k G_{kj}x_k\right)^3} \end{array} \right) \tag{29}$$

where $\frac{\partial \tau_{ij}}{\partial T}=-\frac{\tau_{ij}}{T}$ and $-\frac{\partial G_{ij}}{\partial T}=G_{ij}\left(\alpha_{ij}\frac{\partial \tau_{ij}}{\partial T}\right)$.

$$\frac{\partial \gamma_i}{\partial x_j}=\gamma_i \left(\begin{array}{l} \frac{\left(\tau_{ji}G_{ji}-\tau_{ni}G_{ni}\right)\left(\sum_k G_{ki}x_k+G_{ni}\left(1-\sum_k^{n-1}x_k\right)\right)-\left(G_{ji}-G_{ni}\right)\left(\sum_k^{n-1}\tau_{ki}G_{ki}x_k+\tau_{ni}G_{ni}\left(1-\sum_k^{n-1}x_k\right)\right)}{\left(\sum_k G_{ki}x_k+G_{ni}\left(1-\sum_k^{n-1}x_k\right)\right)^2} \\ +\sum_{m\neq j}\frac{-G_{im}x_m\tau_{im}\left(G_{jm}-G_{nm}\right)}{\left(\sum_k G_{km}x_k+G_{nm}\left(1-\sum_k^{n-1}x_k\right)\right)^2}+\frac{\tau_{ij}G_{ij}\left(\sum_k G_{kj}x_k+G_{nj}\left(1-\sum_k^{n-1}x_k\right)\right)-\left(G_{jj}-G_{nj}\right)\tau_{ij}G_{ij}x_j}{\left(\sum_k G_{kj}x_k+G_{nj}\left(1-\sum_k^{n-1}x_k\right)\right)^2} \\ -\frac{G_{in}\tau_{in}\left(\sum_k G_{kn}x_k+G_{nn}\left(1-\sum_k^{n-1}x_k\right)\right)+G_{in}\tau_{in}\left(1-\sum_k^{n-1}x_k\right)\left(G_{jn}-G_{nn}\right)}{\left(\sum_k G_{kn}x_k+G_{nn}\left(1-\sum_k^{n-1}x_k\right)\right)^2} \\ -\sum_{m\neq j}\left(G_{im}x_m\left\{\left(G_{jm}\tau_{jm}-G_{nm}\tau_{nm}\right)\left(\sum_k G_{km}x_k+G_{nm}\left(1-\sum_k^{n-1}x_k\right)\right)\right.\right. \\ \left.\left.-2\left(G_{jm}-G_{nm}\right)\left(\sum_k^{n-1}\tau_{km}G_{km}x_k+\tau_{nm}G_{nm}\left(1-\sum_k^{n-1}x_k\right)\right)\right\}\Big/\left(\sum_k G_{km}x_k+G_{nm}\left(1-\sum_k^{n-1}x_k\right)\right)^3\right) \\ -\left\{\left(G_{ij}\left(\sum_k^{n-1}\tau_{kj}G_{kj}x_k+\tau_{nj}G_{nj}\left(1-\sum_k^{n-1}x_k\right)\right)+G_{ij}x_j\left(\tau_{jj}G_{jj}-G_{nj}\tau_{nj}\right)\right)\left(\sum_k G_{kj}x_k+G_{nj}\left(1-\sum_k^{n-1}x_k\right)\right)\right. \\ \left.-2G_{ij}x_j\left(G_{jj}-G_{nj}\right)\left(\sum_k^{n-1}\tau_{kj}G_{kj}x_k+\tau_{nj}G_{nj}\left(1-\sum_k^{n-1}x_k\right)\right)\right\}\Big/\left(\sum_k G_{kj}x_k+G_{nj}\left(1-\sum_k^{n-1}x_k\right)\right)^3 \\ -G_{in}\left\{\left(-\left(\sum_k^{n-1}\tau_{kn}G_{kn}x_k+\tau_{nn}G_{nn}\left(1-\sum_k^{n-1}x_k\right)\right)+\left(1-\sum_k^{n-1}x_k\right)\left(\tau_{jn}G_{jn}-\tau_{nn}G_{nn}\right)\right)\right. \\ \left(\sum_k G_{kn}x_k+G_{nn}\left(1-\sum_k^{n-1}x_k\right)\right)-2\left(1-\sum_k^{n-1}x_k\right)\left(\sum_k^{n-1}\tau_{kn}G_{kn}x_k+\tau_{nn}G_{nn}\left(1-\sum_k^{n-1}x_k\right)\right) \\ \left.\left(G_{jn}-G_{nn}\right)\right\}\Big/\left(\sum_k G_{kn}x_k+G_{nn}\left(1-\sum_k^{n-1}x_k\right)\right)^3 \end{array} \right) \tag{30}$$

The partial derivatives of ϑ according to the mole fractions are also difficult to determine, because function ϑ is not known explicitly. However, the implicit function theorem can be applied. T is determined according to Eqs. 4 and 9. Combination of these two equations leads to the criterion

$$\begin{aligned} P\left(x_{\mathrm{A}},x_{\mathrm{B}},T\right)=\gamma_{\mathrm{E}}\left(x_{\mathrm{A}},x_{\mathrm{B}},x_{\mathrm{E}},T\right)x_{\mathrm{E}}p_i^{\circ}\left(T\right)+\sum_{i\in\{A,B\}}\gamma_i\left(x_{\mathrm{A}},x_{\mathrm{B}},x_{\mathrm{E}},T\right)x_i p_i^{\circ}\left(T\right) \\ x_{\mathrm{E}}=1-x_{\mathrm{A}}-x_{\mathrm{B}}. \end{aligned} \tag{31}$$

Table 3 Interval enclosure of a bifurcation point of (RP) at specified $\mathbf{x}_D$

R	[0.6290669441223144, 0.6290836334228516]
x_{acetone}	[0.6932788372039798, 0.6932974338531500]
x_{methanol}	[0.0201442718505859, 0.0201454162597657]
T	[333.1959158182144165, 333.1962019205093384]

Table 4 Interval enclosure of bifurcation points of the (EP) at two reflux ratios

	$R = 4$	$R = 10$
F/V	[0.2063720703125000, 0.2069946289062501]	[0.1578170891437115, 0.1585855111005144]
x_{acetone}	[0.5877075195312502, 0.5881469726562504]	[0.7042266845703127, 0.7047851562500003]
x_{methanol}	[0.0673706054687500, 0.0677490234375001]	[0.0400826140894999, 0.0404432357242396]
T	[333.9262008666992187, 333.9355468750000001]	[332.6806640624999999, 332.6953125000000001]

The differentials of P according to the mole fractions x_A and x_B should be zero, because P is specified as a constant:

$$\gamma_k p_k^\circ - \gamma_E p_E^\circ + \sum_{i\in\{A,B\}} x_i \left(p_i^\circ \left[\frac{\partial \gamma_i}{\partial T} - \frac{\partial \gamma_E}{\partial T} + \frac{\partial \gamma_i}{\partial x_k} - \frac{\partial \gamma_E}{\partial x_k} \right] + \gamma_i \frac{\mathrm{d}p_i^\circ}{\mathrm{d}T} \right) = 0 \quad k \in \{A, B\}. \tag{32}$$

From here, the a derivatives of T are

$$\left.\frac{\partial \vartheta}{\partial x_j}\right|_{\mathbf{x}} = -\frac{\left(\frac{\partial P(x_A, x_B, T)}{\partial x_j}\right)}{\left(\frac{\partial P(x_A, x_B, T)}{\partial T}\right)}. \tag{33}$$

Thus, the bifurcation points of the DAE (RP) can be located by finding the roots of the equation system

$$(2), (5)\text{–}(8), (10), (16), (31) \tag{BRP}$$

and the bifurcation points of the DAE (EP) can be located by finding the roots of the equation system

$$(3), (5)\text{–}(8), (10), (16), (31). \tag{BEP}$$

These equation systems are solved in the same way as SRP and SEP, in Sect. 4.

Computed results are collected in Tables 3 and 4. The numbers shown in these Tables are the interval enclosures of the exact values, respectively, according to the applied model. The upper bounds are shown below the lower bounds; the identical leading digits are underlined for easy comparison.

The interval shown in the first row of Table 3 is interpreted in such a way that the minimum reflux ratio is not higher than 0.6290836334228516, and not lower than

0.6290669441223144. Use of so many digits is meaningless in practice; however, the bounds are valid. The intervals shown in the first row in Table 4 are interpreted in a similar way: The minimum feed ratio of a feasible process at $R = 4$ and $R = 10$ are enclosed in the given intervals.

About 2,186,495 function evaluations were performed to achieve the results of Table 3; 11,104,607 and 7,266,434 evaluations were performed to obtain the results of Table 4 for $R = 4$ and $R = 10$, respectively.

6 Conclusion

Feasible domain of process parameters are difficult to determine in case of batch extractive distillation, an important industrial process. The check of feasibility is based on analyzing the phase maps of DAE models describing the possible composition profiles along the distillation column. The feasible domain is normally explored by tracing the shifts of the singular points in the phase space. The border of the feasible domain is detected by bifurcations.

An interval arithmetic based branch-and-bound optimization tool is applied to analyze phase maps of the DAE models. The root search problems are first transformed to minimum problems with sum of squares as objective function. Using this tool, we are able to reliably find all the singular points of the maps. The tool is also successfully applied to find bifurcation points when the bifurcation criterion is also included in the model.

Bifurcation is detected in the studied problems simply by zero determinant of the linearized system in the singular points. This criterion is expressed in a rather complicated equation system because implicit function theorem has to be applied for determining the Jacobian.

Studying the maps of the acetone (A)–methanol (B)–water (E) system, we find that there are four singular points (two saddles, a stable node, and an unstable node) at high reflux ratios. At total reflux and increasing feed ratio, the two saddles move along the AE and the BE edges, respectively, toward the water vertex (component E); the stable node meets the saddle on the AE edge, and they change stability. At finite reflux ratio, the singular points are found inside the triangle; the stable node and the saddle point initiated from vertex A collide, and bifurcation occurs. Both colliding singular points vanish after the collision, and the phase curves lead out from the triangle through the AE edge.

These results can be successfully applied in exploring the feasible domain of the studied and similar problems without dense computation and visualization of the phase curves. Moreover, the new methodology is a reliable one in contrast to the graphical methodology which is liable to the risk of failing due to insufficient density of the map.

Acknowledgments This research was partially supported by Hungarian National Research Fund (OTKA) grants F 046282, T 048377, T 046822, T 037191, and K 062099.

References

1. Lelkes, Z., Lang, P., Benadda, B., Moszkowicz, P.: Feasibility of extractive distillation in a batch rectifier. AIChE J. **44**, 810–822 (1998)

2. Lelkes, Z., Rév, E., Stéger, Cs., Fonyó, Z.: Batch extractive distillation of maximal azeotrope with middle boiling entrainer. AIChE J. **48**, 2524–2536 (2002)
3. Rév, E., Lelkes, Z., Varga, V., Stéger, Cs., Fonyó, Z.: Separation of minimum boiling binary azeotrope in batch extractive rectifier with intermediate boiling entrainer. Ind. Eng. Chem. Res. **42**, 162–174 (2003)
4. Kunzentsov, Y.A.: Elements of Applied Bifurcation Theory. 2nd ed. Springer, New York (1998)
5. Guckenheimer, J., Holmes, P.: Nonlinear Oscillations, Dynamical Systems and Bifurcations of Vector Fields. Springer, New York (1983)
6. Hammer, R., Hocks, M., Kulisch, U., Ratz, D.: Numerical Toolbox for Verified Computing I. Springer-Verlag, Berlin (1993)
7. Knüppel, O.: PROFIL—Programmer's Runtime Optimized Fast Interval Library. Technische Universität Hamburg, Hamburg (1993)
8. Ratschek, H., Rokne, J.: Computer Methods for the Range of Functions. Ellis Horwood, Chichester (1984)
9. Markót, M.Cs., Csendes, T., Csallner, A.E.: Multisection in Interval Branch-and-Bound Methods for Global Optimization II. Numerical Tests. J. Glob. Opt. **16**, 219–228 (2000)
10. Ratz., D.: Automatische Ergebnisverifikation bei globalen Optimierungsproblemen. Dissertation, Universität Karlsruhe (1992)
11. Csallner, A.E., Csendes, T., Markót, M.Cs.: Multisection in Interval Branch-and-Bound Methods for Global Optimization I. Theoretical Results. J. Glob. Opt. **16**, 371–392 (2000)
12. Brook, A., Kendrick, D., Maereus, A., Raman, R.: GAMS: A User's Guide. GAMS Development Corporation, Washington DC, http://www.gams.com. Cited 19 May 2006 (1998)
13. Drud, A.: CONOPT. Solver Manual. ARKI Consulting and Development A/S, Bagsvaerd, Denmark(2006). http://www.gams.com/dd/docs/solvers/conopt.pdf. Cited 19 May 2006
14. Golubitsky, M., Schaeffer, D.G.: Singularities and Groups in Bifurcation Theory vol. I. Springer, New York (1985)
15. Seydel, R.: Practical Bifurcation and Stability Analysis: From Equilibrium to Chaos. Springer, New York (1994)